Control of Electron Transfer Between the L- and M-Sides of Photosynthetic Reaction Centers

Barbara A. Heller, Dewey Holten, Christine Kirmaier

An aspartic acid residue has been introduced near ring V of the L-side accessory bacteriochlorophyll ($BChl_L$) of the photosynthetic reaction center in a *Rhodobacter capsulatus* mutant in which a His also replaces Leu 212 on the M-polypeptide. The initial stage of charge separation in the G(M201)D/L(M212)H double mutant yields ~70 percent electron transfer to the L-side cofactors, ~15 percent rapid deactivation to the ground state, and ~15 percent electron transfer to the so-called inactive M-side bacteriopheophytin (BPh_M). It is suggested here that the Asp introduced at M201 modulates the reduction potential of $BChl_L$, thereby changing the energetics of charge separation. The results demonstrate that an individual amino acid residue can, through its influence on the free energies of the charge-separated states, effectively dictate the balance between the forward electron transfer reactions on the L-side of the RC, the charge-recombination processes, and electron transfer to the M-side chromophores.

The three-dimensional structures of bacterial photosynthetic reaction centers (RCs) from *Rhodopseudomonas viridis* and *Rhodobacter sphaeroides* (*1*) have revealed an approximately C_2 symmetric arrangement of the L- and M-polypeptides and associated cofactors (Fig. 1). Charge separation begins when the excited singlet state, P*, of the dimer (P) of bacteriochlorophyll (BChl) molecules transfers an electron in ~3 ps to the L-side bacteriopheophytin (BPh_L). The role of the L-side accessory bacteriochlorophyll ($BChl_L$) in this process has not been fully resolved despite intensive efforts focused on this issue (*2*). After formation of $P^+BPh_L^-$, an electron is transferred from BPh_L^- to the primary quinone (Q_A) in ~200 ps. Within experimental uncertainty, the quantum yield of this overall charge separation process is unity.

Explanations for the remarkable unidirectional asymmetry of electron transfer to the L-side cofactors, and the free energy (ΔG) and involvement of $P^+BChl_L^-$ in initial charge separation, have been sought in a wide variety of site-directed mutants. To date, about 15 sites near P, $BChl_L$, $BChl_M$, or BPh_L have been targeted. In some cases, no effective changes from the native photochemistry have been found. Otherwise, two broad classes of mutants can be considered. In the first group, initial electron transfer from P* is perturbed (*3–10*). A slower rate for reduction of BPh_L or an enhanced rate of deactivation of P* to the ground state or both are found, and depending on the balance between these two rates, a reduction in the quantum yield of $P^+BPh_L^-$ formation may result. Electron transfer from BPh_L^- to Q_A in these mutants is similar to that in wild type and takes place quantitatively in 100 to 300 ps. In the second class of mutants, a different pigment is substituted for BPh_L. This substitution was achieved in the Leu to His mutation at M214 of *Rb. sphaeroides* wherein a BChl (denoted β) is incorporated in place of BPh_L—the result of introduction of a His centered over one face of BPh_L (*11*). Chemical methods have been used to substitute pheophytin for BPh_L (*12, 13*). New beta-type RCs have been made in *Rb. capsulatus* (*14*) by substituting His at either L124 or, in special cases, at L121, both of which are over the face of BPh_L opposite to that occupied by M212 (M214 in *Rb. sphaeroides*).

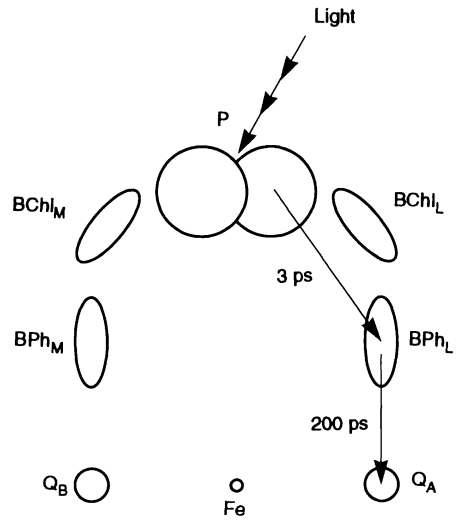

Fig. 1. Schematic representation of the cofactor arrangement in the bacterial photosynthetic reaction center; symbols are defined in the text. In the mutant studied here, BPh_L is replaced with a BChl molecule denoted β.

Electron transfer in beta-type RCs. This second class of mutants is the starting point for the work done here. All of the beta-type (and pheophytin-substituted) RCs reported to date have a common photochemistry (Fig. 2B) that is distinct from the wild-type photochemistry (Fig. 2A) and from that of the first class of mutants. The kinetics and yield of initial electron transfer from P* are largely unperturbed in the beta-type mutants forming, in 5 to 8 ps, a charge-separated transient denoted P^+I^- that is believed to be a mixture (either quantum mechanical or thermal or both) of $P^+\beta^-$ and $P^+BChl_L^-$ (*11–16*). This assessment is consistent with the expectation that $P^+\beta^-$ is at higher ΔG than $P^+BPh_L^-$ in wild type, resulting in increased interaction with $P^+BChl_L^-$. Although the precise nature of P^+I^- in these RCs is not fully resolved, the data are clear in showing that P* → P^+I^- has a yield of ~1. However, subsequent electron transfer from I^- to Q_A is significantly altered, with only a 60 to 80 percent yield of $P^+Q_A^-$ depending on the particular beta-type mutant. Based on this yield, the P^+I^- lifetime, and a simple kinetic branching scheme, one obtains on average an ~500 ps inherent time constant for P^+I^- → $P^+Q_A^-$ electron transfer and an ~900-ps inherent time constant for P^+I^- deactivation (*11–16*). In comparison, wild-type RCs have an ~200-ps time constant for reduction of Q_A and an ~20-ns inherent deactivation time for $P^+BPh_L^-$. Thus, more than just a simple slowing of electron transfer to Q_A, the greatly enhanced inherent rate of P^+I^- → ground state is responsible for the reduced yield of $P^+Q_A^-$ in beta-type RCs.

Construction of the double mutant. Mutations of residues near ring V of the RC pigments have typically demonstrated significant effects on the electronic properties of the chromophores (*4, 8–10, 14, 15*). We have constructed a *Rb. capsulatus* double mutant incorporating the L(M212)H mutation and introducing an Asp (D) residue at M201, which is near ring V of $BChl_L$ (*17*). As expected, we find G(M201)D/L(M212)H RCs have a BChl (β) in place of BPh_L. The predominant differences in the ground-state spectrum of the mutant compared to wild-type RCs (Fig. 3) are essentially identical to those found previously for all other beta-type RCs, and can be associated with the replacement of BPh_L with a BChl. As seen in the inset to Fig. 3, the 543-nm Q_X band of BPh_L is notably absent; the 530-nm Q_X band of BPh_M of course remains. The spectrum also shows reduced BPh Q_Y absorption near 760 nm and increased BChl Q_X and Q_Y absorption near 600 and 780 nm, respectively (*18*). We performed pigment extractions on the mutant and obtained a BChl/BPh pigment ratio of 4.6 ± 0.5 and

The authors are in the Department of Chemistry, Washington University, St. Louis, MO 63130, USA.

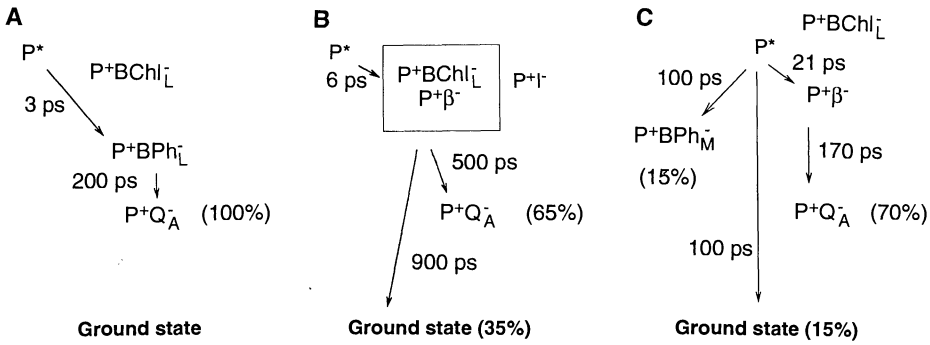

Fig. 2. Summaries of the room-temperature primary photochemistry in (**A**) wild-type RCs, (**B**) normal beta-type RCs, and (**C**) the G(M201)D/L(M212)H mutant. The states are positioned to indicate their relative ΔG ordering. The box enclosing $P^+\beta^-$ and $P^+BChl_L^-$ in (B) denotes that both states are believed to contribute to P^+I^- through thermal equilibration or quantum mechanical mixing or both (and the relative energies of these two basis states may be reversed from that shown). The inherent time constants for the specific processes are calculated from the observed lifetimes and yields. Routes for deactivation to the ground state are not explicitly shown for states whose competing forward electron transfer reactions have yields of ~1.

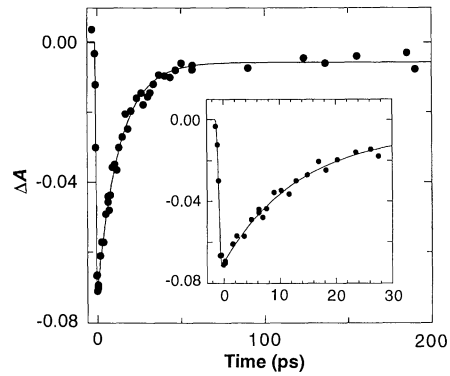

Fig. 5. Decay kinetics of P* stimulated emission between 910 and 920 nm. The solid line is a fit of the data to an exponential plus a constant plus the cross correlation of the pump and probe pulses, giving a P* lifetime of 15 ± 1 ps.

total pigment content of 6.2 ± 0.3. These results, including a pigment ratio ~10 percent lower than the expected value of 5, are essentially identical to those found previously for the other beta-type RCs (*11*, *14*). (We routinely obtain a BChl/BPh ratio of 1.8 for wild-type RCs, a value that also is ~10 percent low.) Side-by-side redox titrations of P were performed on the mutant and wild-type RCs following the procedures given in (9). An oxidation potential of 500 ± 10 mV was found for both the G(M201)D/L(M212)H mutant and wild-type RCs.

Time-resolved spectroscopic studies. The result of ultrafast transient absorption studies on the G(M201)D/L(M212)H mutant are given in Figs. 4 through 8 (*19*). As we describe below, these data demonstrate that the defining beta-type photochemistry (branching at P^+I^- as in Fig. 2B) is negated and restored to wild type. Further, initial charge separation from P* is dramatically altered and yields ~15 percent electron transfer to BPh_M.

Bleaching of the 855-nm ground-state absorption of the dimer P at 1 ps after excitation is shown in Fig. 4. Stimulated emission from P* is manifest as the apparent absorption decrease on the long-wavelength side of the bleaching (for example, near 920 nm). A single exponential fit of the decay of the stimulated emission returns a P* lifetime of 15 ± 1 ps (Fig. 5). At 50 ps, stimulated emission is no longer seen and the magnitude of P bleaching is clearly reduced compared to the initial value. This decay of P bleaching in the G(M201)D/L(M212)H mutant indicates partial deactivation of P* to the ground state, corresponding to a decrease in the quantum yield of charge separation. Decay of P bleaching (loss of quantum yield) does not occur during the P* lifetime in wild-type RCs or in any other beta-type RC (*11*, *14*, *15*). A yield of ~15 percent for decay of P* to the ground state in the mutant is calculated from the extent of the decay in P bleaching between 840 and 850 nm. There also may be an additional decrease of a few percent in bleaching of P at 2 ns, the origin of which is discussed below.

Between 600 and 700 nm, where the anions of both BPh and BChl have characteristic absorption bands, the initial positive and featureless spectrum of P* gives way to the P^+I^- transient absorption shown at 50 ps in Fig. 6 (inset). This absorption decays with a time constant of 170 ± 20 ps (Fig. 6). Because there is no decay of P bleaching on this time scale (within a few percent), 170 ps reflects the time constant for $P^+I^- \rightarrow P^+Q_A^-$ electron transfer. Formation of $P^+Q_A^-$ is further evidenced in the spectral data in the 750- to 850-nm Q_Y region.

Transient spectra for G(M201)D/L(M212)H RCs in the Q_X region are shown in Fig. 7A. A bleaching centered near 530 nm is clearly resolved in the spectrum taken after P* decay at 50 ps and contrasts with the featureless spectrum of P* observed at 1 ps. Because BPh_M is responsible for the ground-state absorption at this wavelength, we assign the 530-nm feature as bleaching of the Q_X

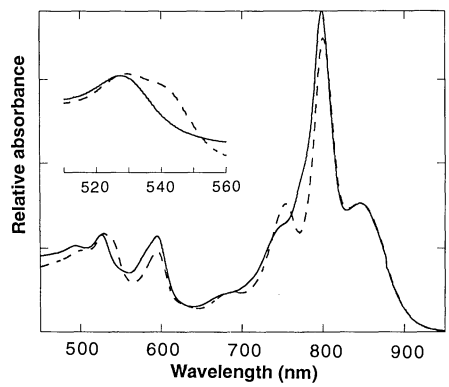

Fig. 3. Ground-state absorption spectra of *Rb. capsulatus* G(M201)D/L(M212)H RCs (solid) and wild-type RCs (dashed) at 298 K.

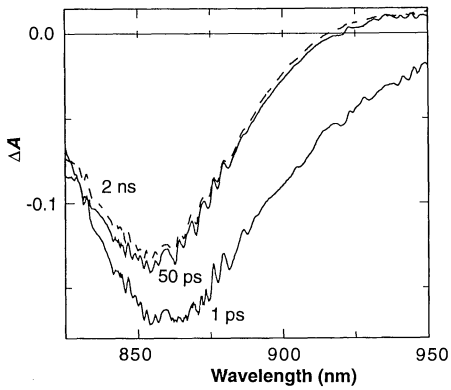

Fig. 4. Transient difference spectra for G(M201)D/L(M212)H RCs at 285 K in the region of the ground-state absorption of P at the indicated times after excitation with a 150-fs flash at 582 nm.

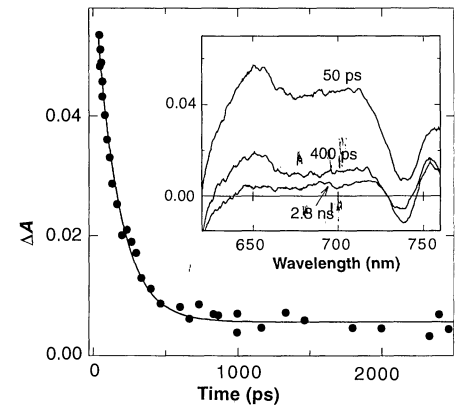

Fig. 6. Decay of the transient absorption (inset) due to I^- at 665 nm along with a fit (as in Fig. 5), giving a P^+I^- lifetime of 170 ± 20 ps. The same time constant within experimental error is found between 630 and 700 nm.

band of this chromophore due to the formation of $P^+BPh_M^-$ (*20*). At 2.3 ns, the magnitude of the 530-nm bleaching is diminished but persists. Wild-type spectra of $P^+BPh_L^-$ (20 ps) and $P^+Q_A^-$ (2.3 ns) are shown in Fig. 7B for comparison. In Figs. 7C, 7D, and 8, we compare spectra for our double mutant, wild-type, and beta-type RCs through the Q_X bands of both the BPhs and BChls. On the basis of comparison of the magnitude of 530-nm bleaching in G(M201)D/L(M212)H RCs to that at 543 nm in wild-type RCs (Fig. 7C), we estimate the yield of P^+BPh_M to be ~15 percent in the mutant.

Formation of $P^+BPh_M^-$ is supported by two other observations. First, in the anion region, a small residual absorption between 640 and 680 nm remains after the decay of the main absorption due to the L-side P^+I^- (2.3-ns spectrum in Fig. 6). BPh_M^- is expected to absorb in this region, whereas $P^+Q_A^-$ does not (*21*). Second, the bleaching at 530 nm shows a small decay by several nanoseconds (Fig. 7A). We expect $P^+BPh_M^-$ to decay over several to tens of nanoseconds through charge recombination to the ground state (*22*). As noted above (Fig. 4), a few percent decay of P bleaching is also (barely) resolved at 2.3 ns compared to 50 ps (*23*). These observations are offered here not as unambiguous points of evidence but rather as support for the formation of $P^+BPh_M^-$ and in combination with the clear 530-nm bleaching contribute to a compelling assignment.

Modeling electron transfer and energetics. Collectively, the spectral and kinetic data presented here evoke the description of the photochemistry in G(M201)D/L(M212)H RCs illustrated in Fig. 2C. First, the normal beta-type photochemistry depicted in Fig. 2B is clearly negated. Rather than fast quantitative initial charge separation $P^* \rightarrow P^+I^-$, and subsequent branched P^+I^- decay to give a reduced $P^+Q_A^-$ yield and significant ground-state recovery, the photochemistry in G(M201)D/L(M212)H RCs is branched instead at P* and is followed by unperturbed electron transfer from I^- to Q_A. Specifically, $P^+I^- \rightarrow P^+Q_A^-$ proceeds with effectively wild-type kinetics (~170 ps compared to the native ~200 ps) and with no significant loss of quantum yield (*23*). The combination of spectral and kinetic data in the anion region and the essentially constant magnitude of P bleaching on the time scale of electron transfer to Q_A clearly establish this picture. This is an extraordinary reversal of the normal beta-type photochemistry. This is a significant result, even in the absence of finding electron transfer to BPh_M, and gives direct insight into factors that dictate the balance between the charge-separation and charge-recombination reactions on the photoactive side of the RC.

The model that emerges is that the combined participation of $P^+BChl_L^-$ and $P^+\beta^-$ in P^+I^- in the normal beta-type RCs (Fig. 2B) has been altered in the G(M201)D/L(M212)H mutant. Our working hypothesis to explain our results is that the Asp at M201, which is positioned within a few angstroms of ring V of $BChl_L$ (*1*), has raised the ΔG of $P^+BChl_L^-$, as illustrated in Fig. 2C. Such a change in the ΔG of this state would be most readily explained if Asp M201 is charged (*24*). This shift in turn would increase the ΔG between $P^+BChl_L^-$ and $P^+\beta^-$, resulting in reduced mixing (quantum mechanical or thermal or both) of these states compared to the situation in normal beta-type RCs. This would affect the rates of electron transfer ($P^+I^- \rightarrow P^+Q_A^-$) and charge recombination ($P^+I^- \rightarrow$ ground state) in precisely the ways we have observed (*25*). In effect, the P^+I^- transient in the G(M201)D/L(M212)H mutant has less the character of $P^+BChl_L^-$ and more that of $P^+\beta^-$ compared to the previously reported β-containing RCs (*11, 14, 15*).

The ΔG of $P^+BChl_L^-$ in wild-type RCs is not known. We argue that the combined results on our new double mutant, the previous beta-type mutants (*11, 14, 15*), and pheophytin-substituted RCs (*12, 13*) present a powerfully consistent picture that $P^+BChl_L^-$ is slightly below P*. Some calculations place $P^+BChl_L^-$ very close to P* in wild-type RCs (*26*), and an ordering with the former slightly lower is indicated in studies that have offered evidence for a contribution from an initial two-step charge separation sequence, $P^* \rightarrow P^+BChl_L^- \rightarrow P^+BPh_L^-$, in wild-type RCs (*5, 6, 27, 28*). In order to effect the restoration of the native $P^+I^- \rightarrow P^+Q_A^-$ dynamics (kinetics and yield) in the G(M201)D/L(M212)H mutant, the ΔG gap between $P^+BChl_L^-$ and $P^+\beta^-$ must be considerably greater than in

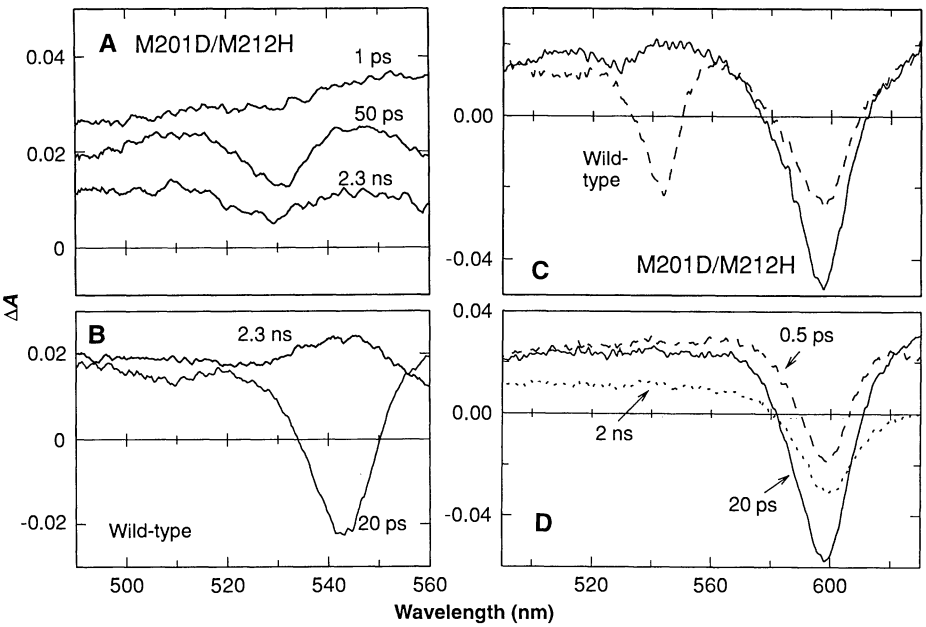

Fig. 7. Absorption changes in the Q_X region at 285 K. (**A** and **B**) Transient spectra in the region of BPh Q_X absorption acquired with 150-fs flashes at 582 nm. (**C** and **D**) Data acquired with 150-fs flashes at 860 nm, and probing through the region of Q_X absorption of both the BPhs and BChls. The 50-ps and 2.3-ns spectra in (A) for G(M201)D/L(M212)H RCs show bleaching of the 530-nm absorption of BPh_M. For comparison, bleaching of the BPh_L absorption at 543 nm in wild-type RCs is illustrated in the 20-ps $P^+BPh_L^-$ spectrum in (B); the 2.3-ns spectrum is for state $P^+Q_A^-$. The data in (C) were obtained with samples of wild-type and G(M201)D/L(M212)H RCs having identical concentration (same absorption through the long-wavelength band of P) studied under identical conditions of excitation. The spectra shown were acquired at times after P* decay corresponding to about four P* lifetimes in the respective samples (~15 ps for wild type and ~55 ps for the mutant). In this way, comparison of the integrated bleaching at 530 nm in the mutant with that at 543 nm in wild type yields a good estimate of the yield (~15 percent) of $P^+BPh_M^-$ in the mutant. The absolute accuracy of this yield estimate depends, of course, on the relative oscillator strengths of BPh_L and BPh_M absorptions; these were taken to be the same as indicated in the ground-state spectra in Fig. 3 (inset). Representative data are shown in (D) for beta-type RCs required under the same conditions (matched sample concentration and identical excitation conditions) used for (C). The spectra for P* (0.5 ps), P^+I^- (20 ps), and $P^+Q_A^-$ (2 ns) acquired for *Rb. sphaeroides* L(M214)H RCs are essentially identical to those obtained for all six beta-type mutants investigated in our laboratory, two from *Rb. sphaeroides* and four from *Rb. capsulatus* (*11, 14, 15*); see also Fig. 8. The utility of a beta-type background in assaying for BPh_M bleaching at 530 nm is apparent from the spectra in (D). The data in (B) and (C) illustrate the difficulties that arise in cleanly resolving very small yields of $P^+BPh_M^-$ in the presence of substantial BPh_L bleaching in wild-type or other BPh_L-containing RCs at room temperature.

normal beta-type RCs, approaching the gap between $P^+BChl_L^-$ and $P^+BPh_L^-$ in wild-type RCs. On this basis, we speculate that the effect of the Asp is to raise $P^+BChl_L^-$ by ~100 meV or more, probably putting it above P*, as suggested in Fig. 2C (*29*). We have independent support that the presence of an Asp can cause such a large modulation of the energetics in another mutant, in which we have introduced an Asp near ring V of BPh_L (*30*). These RCs have the wild-type pigment content (BPh_L is still present), yet they display the defining charge-separation properties of a beta-type RC. P* decays in ~5 ps to yield P^+I^- with no loss of quantum yield, but this is followed by branching photochemistry with P^+I^- decaying partially by electron transfer to yield $P^+Q_A^-$ and partially by charge recombination to yield the ground state. Again, the working model is that the Asp residue, perhaps charged, raises the ΔG of $P^+BPh_L^-$ so that, like $P^+\beta^-$ in the original beta-type RCs, $P^+BPh_L^-$ is at high enough energy to mix with $P^+BChl_L^-$ and thereby afford the observed beta-like photochemistry. These results corroborate those reported here on the G(M201)D/L(M212)H double mutant and support further the models shown in Fig. 2, B and C.

A significant increase in the ΔG of $P^+BChl_L^-$ should perturb electron transfer to the L-side, no matter whether the mechanism of initial electron transfer (in wild-type or normal beta-type RCs) involves two steps, superexchange, or both. Indeed, we observe a lengthened P* lifetime and a functional branching of the photochemistry at this initial excited state in the G(M201)D/L(M212)H mutant. A similar effective competition between P* → ground state and P* → L-side charge separation, or at a minimum a slowing of initial charge separation, has been observed in a number of other mutants (*3–10*). However, to our knowledge, the clean spectral evidence presented here in the G(M201)D/L(M212)H mutant for electron transfer to BPh_M has not been found in previous studies of other RCs.

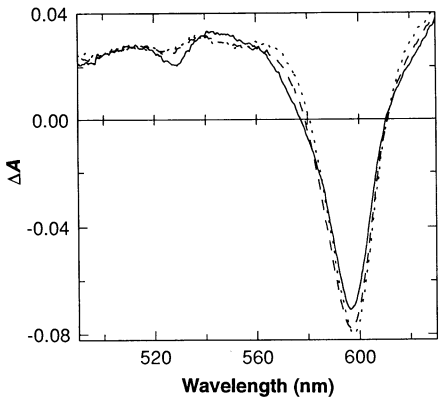

Fig. 8. Comparison of spectra of P^+I^- at four P* 1/*e* decay times for three β-containing RCs: *Rb. sphaeroides* L(M214)H (dotted), *Rb. capsulatus* L(M212)H (dashed), G(M201)D/L(M212)H (solid). These spectra were acquired using slightly greater concentrations and slightly more excitation intensity in order to obtain somewhat larger absorption changes than in Fig. 7. There may be evidence for a small bleaching of the 530-nm absorption of BPh_M in the two single mutants ~2.5 times smaller than that observed for the double mutant.

Rate constants for electron transfer and deactivation. Based on the measured 15-ps P* lifetime and the yields of its photoproducts, we estimate the following values for the inherent time constants in G(M201)D/L(M212)H RCs: P* → ground state ≃ 100 ps; P* → P^+I^- (the L-side) ≃ 20 ps; and P* → $P^+BPh_M^-$ ≃ 100 ps (*31*). At a qualitative level, the simplest explanation for such a substantial slowing of electron transfer to the L-side is if $P^+BChl_L^-$ is now at higher ΔG than P*, as discussed above, thereby diminishing or eliminating a contribution of a two-step mechanism to the initial stage of charge separation. Low-temperature studies and theoretical analyses should provide insights into how the relative contributions of the superexchange and two-step mechanisms have been modulated in this mutant. Such analyses have been carried out for wild-type RC and the M208 mutants (*6, 27*), but are beyond the scope of the present work. The ~100 ps values for P* → ground state and P* → $P^+BPh_M^-$ compare reasonably well with what is known or might be expected but provoke brief comment. An inherent ~100 ps P* deactivation time is slightly shorter than the 150 to 250 ps values obtained previously (*32, 33*). We can speculate that a charge at M201 might impart some charge asymmetry in P*, thereby shortening its inherent deactivation. In this regard, the BChl-BPh heterodimers have ~$(30\ ps)^{-1}$ internal conversion rates (*3*).

A $(100\ ps)^{-1}$ rate for P* → $P^+BPh_M^-$ is about a factor of 30 slower than the ~$(3\ ps)^{-1}$ rate of P* → $P^+BPh_L^-$ in wild-type RCs. This 30/1 ratio is comparable to a lower limit of 25/1 suggested for *Rb. sphaeroides* RCs at 20 K (*34*) and is smaller than the lower limit of 200/1 estimated for *Rps. viridis* RCs at 90 K (*35*). Although these values are reasonably consistent in view of the differences in conditions, the question naturally arises as to whether electron transfer to the M-side is somewhat enhanced in the G(M201)D/L(M212)H mutant. We mention this possibility, even in the absence of a clear mechanism, because an ~100-ps time constant for P* → $P^+BPh_M^-$ in wild-type RCs necessarily would mean there is, in fact, a few percent formation of $P^+BPh_M^-$ in the native system. Although such a yield is not typically considered, neither is it clear it could be unambiguously resolved, at least at room temperature. Similarly, a $(100\ ps)^{-1}$ rate for P* → $P^+BPh_M^-$ together with a 5 to 8 ps P* lifetime in typical beta-type RCs, corresponds to a 5 to 8 percent yield of electron transfer to BPh_M. Such a yield of $P^+BPh_M^-$ is close to the limit of detectability and might be evidenced in the spectra of Fig. 8.

There are a number of other mutants that have P* lifetimes significantly longer than in wild type, and the similar question may be asked as to why in these mutants electron transfer to BPh_M has not been observed. Two reasons may be considered. First, in essentially all of these mutants the oxidation potential of P is changed (*3, 5–10*), resulting in a uniform shift in the ΔGs of all the charge-separated states on both the L- and M-sides. Second, except for the D_{LL} mutant (*33*), these RCs retained the native BPh_L pigment, rendering it difficult to resolve unambiguously any small yield of $P^+BPh_M^-$ through transient bleaching in the BPh Q_X region. In contrast, the G(M201)D/L(M212)H mutant offers a clean spectral window to probe for electron transfer to BPh_M, and the Asp at M201 clearly has altered the ΔG of $P^+BChl_L^-$. This latter factor, either alone or perhaps in combination with an as yet undefined effect on the M-side energetics, has changed the balance of the competitive decay pathways from P* sufficiently to allow for the formation of $P^+BPh_M^-$ observed here.

Modulation of the directionality and yield of charge separation. The observation of electron transfer to BPh_M clearly has profound implications and goes a long way toward understanding one of the most enigmatic properties of the RC, namely, the native unidirectionality of electron transfer. Considerations have been given to numerous structural and energy contributions to global and specific asymmetries that would influence the Franck-Condon and electronic factors for electron transfer through the two branches (*1, 26, 36–39*). One of these contributions is that the balance between electron transfer to BPh_L versus BPh_M is substantially controlled by precisely positioned, and not necessarily greatly differing, ΔGs of $P^+BChl_M^-$ and $P^+BChl_L^-$, with the latter very near and probably below P* in the native protein (*26*). Our results bear out this point of view. The way now seems clear, in principle, to further enhance electron transfer to the M-side of the RC at the expense of the L-side by key positioning of charged amino acids, possibly in conjunction with adding or deleting hydrogen bonds. Based on our results and the body of work on modified RCs, we now should have the ability to alter at will the balance between the forward and reverse charge separation reactions, which along with the competition of electron transfer to the M-side, ultimately dictate the overall yield of charge separation in the photosynthetic reaction center.

REFERENCES AND NOTES

1. H. Michel, O. Epp, J. Deisenhofer, *EMBO J.* **5**, 2445 (1986); H. Komiya, T. O. Yeates, D. C. Rees, J. P. Allen, G. Feher, *Proc. Natl. Acad. Sci. U.S.A.* **85**, 9012 (1988); O. El-Kabbani, C. H. Chang, D. M. Tiede, J. Norris, M. Schiffer, *Biochemistry* **30**, 5361 (1991); U. Ermler, G. Fritzsch, S. K. Buchanan, H. Michel, *Structure* **2**, 925 (1994); J. Deisenhofer, O. Epp, I. Sinning, H. Michel, *J. Mol. Biol.* **246**, 429 (1995).
2. For reviews of the primary photochemistry, see *The Photosynthetic Reaction Center*, J. Deisenhofer and J. R. Norris, Eds. (Academic Press, New York, 1993), vol. 2.
3. C. Kirmaier, D. Holten, E. J. Bylina, D. C. Youvan, *Proc. Natl. Acad. Sci. U.S.A.* **85**, 7562 (1988); L. M. McDowell, D. Gaul, C. Kirmaier, D. Holten, C. C. Schenck, *Biochemistry* **30**, 8315 (1991); L. Laporte, C. Kirmaier, C. C. Schenck, D. Holten, *Chem. Phys.* **176**, 615 (1993).
4. E. J. Bylina, C. Kirmaier, L. McDowell, D. Holten, D. Youvan, *Nature* **336**, 182 (1988).
5. U. Finkele, C. Lauterwasser, W. Zinth, K. A. Gray, D. Oesterhelt, *Biochemistry* **29**, 8517 (1990); Y. Jia *et al., J. Phys. Chem.* **97**, 13180 (1993).
6. V. Nagarajan, W. W. Parson, D. Davis, C. C. Schenck, *Biochemistry* **32**, 12324 (1993).
7. A. K. W. Taguchi *et al., ibid.* **31**, 10345 (1992).
8. The *Rb. sphaeroides* G(M203)D single mutant, equivalent to G(M201)D in *Rb. capsulatus*, has been reported; J. C. Williams *et al., Biochemistry* **31**, 11209 (1992). Differences from the wild-type photochemistry were observed for that mutant, but the effects are not as large as those reported here.
9. H. A. Murchison *et al., Biochemistry* **32**, 3498 (1993).
10. N. W. Woodbury *et al., ibid.* **33**, 8101 (1994).
11. C. Kirmaier, D. Gaul, R. DeBey, D. Holten, C. C. Schenck, *Science* **251**, 922 (1991).
12. A. Y. Shkurapatov and V. A. Shuvalov, *FEBS Lett.* **322**, 168 (1993).
13. S. Schmidt *et al., Chem. Phys. Lett.* **223**, 116 (1994).
14. B. Heller, D. Holten, C. Kirmaier, *Biochemistry* **34**, 5294 (1995).
15. C. Kirmaier, L. Laporte, C. C. Schenck, D. Holten, *J. Phys. Chem.* **99**, 8903 (1995); *ibid.*, p. 8910.
16. M. Bixon, J. Jortner, M. E. Michel-Beyerle, in *The Photosynthetic Bacterial Reaction Center II*, J. Breton and A. Vermeglio, Eds. (Plenum, New York, 1992), p. 291.
17. The general molecular biological techniques (plasmids, strains, and so forth) used to make *Rb. capsulatus* mutants, and methods for RC isolation and purification are described in detail elsewhere (*14*). Specifically for the G(M201)D/L(M212)H mutant the oligo used to effect the M201D mutation changed GGC (Gly) to GAT (Asp) and, for screening purposes, also contained a silent mutation at Ser M203 (TCG → TCA) that removed a Pvu I restriction enzyme recognition site. The oligo for the M212H mutation changed CTC (Leu) to CAC (His) and also incorporated a silent mutation at Ser M210 (TCG → AGC) that added a Bss HII recognition site.
18. The 285 K absorption spectrum of G(M201)D/L(M212)H RCs also reveals a shoulder on the short-wavelength side of the Q_X absorption of the BChls that is partially resolved at 77 K and that is not seen in L(M212)H RCs or other normal beta-type mutants (*11, 14, 15*). This perturbation likely reflects the interaction of Asp M201 with $BChl_L$.
19. Femtosecond transient absorption studies at 285 K were carried out basically as described in C. Kirmaier and D. Holten, *Biochemistry* **30**, 609 (1991). RCs having A = 1 to 2 at 800 nm were contained in an ice-cooled reservoir and flowed through a 2-mm pathlength cell. The RCs were excited at 10 Hz by ~150-fs excitation flashes at 582 nm from an amplified synchronously pumped laser or by ~150-fs excitation flashes at 860 nm from a regeneratively amplified Ti:sapphire laser (all from Spectra Physics or Positive Light). The excitation intensity was adjusted so that ≤30 percent of the RCs were excited. The absorption changes reported were the average of data acquired using ~300 flashes and have typical resolution in ΔA of ~0.005.
20. In analyzing the spectral data, we have considered simple electrochromic bandshifts on either BPh_M or carotenoid; however, a bandshift should result in a positive-going wing corresponding in general shape and amplitude to the negative-going feature at 530 nm. Because such a positive feature is not apparent in the spectra, we believe the feature at 530 nm to be a bleaching. We also note that both of the carotenoids that may be present, spheroidene and spheroidenone, have three absorption peaks of comparable intensity spaced by ~1350 cm^{-1}; [R. J. Cogdell and H. A. Frank, *Biochem. Biophys. Acta* **895**, 63 (1987); D. S. Gottfried, M. A. Steffen, S. G. Boxer, *ibid.* **1059**, 76 (1991)]. The maxima for spheroidene in RCs are near 430, 470, and 500 nm. The absorption of spheroidenone in the RC more closely underlies the BPh Q_X region with the three absorption bands coalescing into a very broad relatively featureless absorption from ~450 to ~550 nm. With these spectral characteristics in mind, the observed single absorption decrease at 530 nm is not readily reconciled with carotenoid. Other alternative explanations for the absorption decrease we observe at 530 nm would have to have novel origins outside current understanding of the spectroscopy and dynamics of the RC.
21. BPh_M^- has been trapped in *Rb. sphaeroides* RCs under continuous illumination in the presence of redox agents; B. Robert, D. M. Tiede, M. Lutz, *FEBS Lett.* **183**, 326 (1985); K. A. Gray, J. Wachtveitl, D. Oesterhelt, *Eur. J. Biochem.* **207**, 723 (1992). This anion has a broad absorption band between 610 and 650 nm. The transient spectrum of $P^+Q_A^-$ (like the absorption difference spectrum of P^+) has $\Delta A \sim 0$ between 620 and 670 nm and a weak positive absorption between 680 and 720 nm; C. Kirmaier, D. Holten, W. W. Parson, *Biochim. Biophys. Acta.* **810**, 49 (1985).
22. The samples used in this work were assayed for Q_B content by following the millisecond to seconds kinetics of P bleaching decay. After a 10-ns, 600-nm flash, P bleaching at 850 nm was found to decay ≥95% with a time constant (~200 ms) that indicates $P^+Q_A^-$ charge recombination. $P^+Q_B^-$ would be expected to decay on the time scale of a few seconds. These results indicate that the samples are essentially devoid of Q_B, as is the case for standard preparations of RCs from wild-type and other mutant strains. Hence, we expect that $P^+BPh_M^-$ will decay by charge recombination. Based on the range of decay times observed for $P^+BPh_L^-$ (in wild-type RCs) or P^+I^- (in beta-type RCs), we expect this decay will occur on the time scale of 1 to 20 ns. The exact lifetime and decay pathways of $P^+BPh_M^-$ are, of course, unknown at present.
23. Another possible source of a few percent P bleaching decay between 50 ps and 2 ns is charge recombination of the L-side P^+I^- transient. In other words, there could be a residual amount of "beta-type" branching of electron transfer at this state. The small amplitude of P bleaching recovery and the ~3 ns time limit of the transient absorption spectrometer preclude measurement of the kinetics of this bleaching decay. Although we suggest the P bleaching recovery between 50 ps and 2 ns is more likely due to $P^+BPh_M^-$ charge recombination, both processes could be occurring simultaneously and independently. In any case, if there is some beta-type photochemistry occurring due to interaction between $P^+\beta^-$ and $P^+BChl_L^-$, it represents only a few percent of the decay of P^+I^-. Because this would affect only marginally the data analysis and model for the photochemistry in our mutant, we have ignored this possibility and consider $P^+I^- \rightarrow P^+Q_A^-$ to proceed with 100% yield.
24. A negatively charged Asp at M201 would almost certainly destabilize $BChl_L^-$ and raise the ΔG of $P^+BChl_L^-$. Calculations indicate that a charge near ring V of a BChl should primarily perturb the Q_Y band of the molecule; J. Eccles and B. Honig, *Proc. Natl. Acad. Sci. U.S.A.* **80**, 4959 (1983); L. K. Hanson, J. Fajer, M. C. Thompson, M. C. Zerner, *J. Am. Chem. Soc.* **109**, 4728 (1987). The effects of nearby charged amino acids on the absorption spectrum of RC pigments is largely unexplored experimentally, and the effects should be sensitive to the exact location of the charged group. Here we, in fact, find that the major perturbation observed in the ground-state absorption spectrum of G(M201)D/L(M212)H RCs is in the Q_X region of the BChls, where a new peak is observed on the blue side of the 600-nm BChl Q_X manifold. Assuming this represents a blue shift of the Q_X band of $BChl_L$ we note that this blue shift is opposite to the red shift expected if Asp were protonated and forming a hydrogen bond to the ring V keto group of $BChl_L$. A red-shifted Q_X band has been documented for formation of a hydrogen bond to the ring V keto group of both BPh_L and β (*4, 15*). Also, the addition of a hydrogen bond should lower the ΔG of $P^+BChl_L^-$, which is opposite to the direction deduced from the perturbed photochemistry. Hence, if the Asp is protonated, its influence on $BChl_L$ would appear to be predominantly through a mechanism different than expected for hydrogen bonding. We also note that studies on myoglobin mutants suggest that a charged Asp or Glu, as well as an uncharged Asn, placed nearby a tetrapyrrole can significantly affect its redox potential without there being concomitant large effects on the optical spectra; R. Varadarajan, D. G. Lambright, S. G. Boxer *Biochemistry* **28**, 3771 (1989).
25. In the simplest terms, a diminished involvement of $P^+BChl_L^-$ compared to $P^+\beta^-$ in P^+I^- effectively moves the unpaired electron density in the reduced acceptor complex closer to Q_A and farther from P^+, thereby enhancing electron transfer and diminishing charge recombination in the double mutant. This is just the opposite of the effect that has been observed and discussed in similar terms with respect to the increased involvement of $P^+BChl_L^-$ in beta-type RCs compared to wild-type (*11, 14, 15*). Thus, we expect similar electronic couplings for electron transfer from $I^-(\beta^-)$ to Q_A in the double mutant and from BPh_L^- to Q_A in wild-type RCs, but with ΔG for the reaction larger by 100 to 200 meV in the mutant. Because the ΔG in wild-type RCs appears to be slightly smaller or comparable to the reorganization energy, and based on current understanding of the relation between rate and ΔG for this process [M. Gunner and P. L. Dutton, *J. Am. Chem. Soc.* **111**, 3400 (1989); L. Laporte, C. Kirmaier, C. C. Schenck, D. Holten, *Chem. Phys.*, in press], we expect the rate of electron transfer to Q_A to be similar in the double mutant and the native system, as is observed.
26. W. W. Parson, Z. T. Chu, A. Warshel, *Biochim. Biophys. Acta* **1017**, 251 (1990).
27. M. Bixon, J. Jortner, M. E. Michel-Beyerle, *ibid.* **1056**, 301 (1991); C.-K. Chan *et al., Proc. Natl. Acad. Sci. U.S.A.* **88**, 11202 (1991).
28. S. V. Chekalin, Y. A. Matveetz, A. Y. Shkuropatov, V. A. Shuvalov, A. P. Yartzev, *FEBS Lett.* **216**, 245 (1987); T. Arlt *et al., Proc. Natl. Acad. Sci. U.S.A.* **90**, 11757 (1993); S. Maiti *et al., ibid.* **91**, 10360 (1994).
29. A number of studies suggest that $P^+BChl_L^-$ lies very near and probably slightly below P^{*} in free energy in wild-type RCs (*5, 6, 11–16, 26–28*). In modeling the results on beta-type mutants, M208 mutants, and pheophytin-substituted RCs, $P^+BChl_L^-$ typically is placed ~70 meV below P* (*6, 13, 15, 16*). $P^+BPh_L^-$ is typically placed ~250 meV below P* [R. A. Goldstein, L. Takiff, S. G. Boxer, *Biochim. Biophys. Acta* **934**, 253 (1988); A. Ogrodnik, A. Keupp, M. Volk, G. Aumeier, M. E. Michel-Beyerle, *J. Phys. Chem.* **98**, 3432 (1994)] and thus ~180 meV below $P^+BChl_L^-$, although it has been suggested that $P^+BPh_L^-$ initially may be at somewhat higher ΔG (*10*). In normal beta-type RCs, $P^+\beta^-$ and $P^+BChl_L^-$ are thought to be essentially isoenergetic (*14, 15*). Taking all of these values into consideration, $P^+BChl_L^-$ must be increased in ΔG in G(M201)D/L(M212)H RCs by up to ~180 meV in order for this state to lie above $P^+\beta^-$ by about the same amount as it is above $P^+BPh_L^-$ in wild-type RCs. Considering the uncertainties in all of these values, we conservatively estimate that the effect of Asp M201 is to increase the ΔG of $P^+BChl_L^-$ by ~100 meV or more in the double mutant. Assuming that the estimate for the position of this state in wild-type RCs is correct, then this shift will likely put $P^+BChl_L^-$ above P*. This possibility is indicated in Fig. 2C.
30. B. A. Heller, D. Holten, C. Kirmaier, in preparation.
31. The estimates for the rate constants for the decay routes of P* may change somewhat if a model including the reverse reactions is utilized. Such analysis will be more meaningful when applied to a larger data set incorporating low-temperature measurements.
32. C. C. Schenck, W. W. Parson, D. Holten, M. W. Windsor, *Biochim. Biophys. Acta* **635**, 383 (1981).
33. J. Breton, J.-L. Martin, J. C. Lambry, S. J. Robles, D. C. Youvan, in *Reaction Centers of Photosynthetic Bac-*

teria, M. E. Michel-Beyerle, Ed., *Springer Series in Biophysics Part 6* (Springer, New York, 1990), p. 293.
34. M. Bixon, J. Jortner, M. E. Michel-Beyerle, A. Ogrodnik, *Biochim. Biophys. Acta* **977**, 273 (1989).
35. E. C. Kellogg, S. Kolaczkowski, M. R. Wasielewski, D. M. Tiede, *Photosynthesis Res.* **22**, 47 (1989).
36. T. O. Yeates, H. Komiya, D. C. Rees, J. P. Allen, G. Feher, *Proc. Natl. Acad. Sci. U.S.A.* **84**, 6438 (1987); M. Losche, G. Feher, M. Y. Okamura, *ibid.*, p. 7537.
37. M. A. Stephan, K. Lao, S. G. Boxer, *Science* **264**, 810 (1994); D. J. Lockhart and S. G. Boxer, *Proc. Natl. Acad. Sci. U.S.A.* **85**, 107 (1988); V. Palaniappan and D. Bocian, *J. Am. Chem. Soc.* **117**, 3647 (1995).
38. M. E. Michel-Beyerle *et al.*, *Biochim. Biophys. Acta* **932**, 52 (1988); P. O. J. Scherer and S. F. Fischer, *Chem. Phys. Lett.* **131**, 115 (1989); R. Friesner and Y. Won, *Biochem. Biophys. Acta* **977**, 99 (1989).
39. M. A. Thompson and M. C. Zerner, *J. Am. Chem. Soc.* **113**, 8210 (1991); M. Marchi, J. N. Gehlen, D. Chandler, M. Newton, *ibid.* **115**, 4178 (1993). These calculations and those in (*26*) consistently place the states on the M-side at higher ΔG than the corresponding states on the L side, and place $P^+BChl_M^-$ above P* in keeping with the native photochemistry.
40. Supported by grant MCB-9405248 from the National Science Foundation and by an Individual National Research Service Award to B.A.H. from the National Institutes of Health. We thank J. Babcock, D. Bocian, and S. Boxer for helpful comments on an early version of the manuscript and D. Daly for assistance with the RC preparations.

5 April 1995; accepted 12 July 1995

Crystal Structure of a Conserved Protease That Binds DNA: The Bleomycin Hydrolase, Gal6

Leemor Joshua-Tor,* H. Eric Xu,† Stephen Albert Johnston, Douglas C. Rees

Bleomycin hydrolase is a cysteine protease that hydrolyzes the anticancer drug bleomycin. The homolog in yeast, Gal6, has recently been identified and found to bind DNA and to act as a repressor in the Gal4 regulatory system. The crystal structure of Gal6 at 2.2 Å resolution reveals a hexameric structure with a prominent central channel. The papain-like active sites are situated within the central channel, in a manner resembling the organization of active sites in the proteasome. The Gal6 channel is lined with 60 lysine residues from the six subunits, suggesting a role in DNA binding. The carboxyl-terminal arm of Gal6 extends into the active site cleft and may serve a regulatory function. Rather than each residing in distinct, separable domains, the protease and DNA-binding activities appear structurally intertwined in the hexamer, implying a coupling of these two activities.

Bleomycin is a small glycometallopeptide produced by *Streptomyces verticillus* that is used as an anticancer drug because of its ability to catalytically cleave double-stranded DNA (*1*). The endogenous enzyme, bleomycin hydrolase (BH), is a cysteine protease that detoxifies bleomycin by hydrolysis of an amide group (*2*). The amounts of this enzyme in the cell limit the effectiveness of the drug, because cancer cells with increased expression of BH are resistant to drug treatment, and because tissues that naturally contain small amounts of BH (skin and lung) are especially sensitive to toxic side effects of bleomycin (*3*).

BH is present in mammals, birds, and reptiles in all tissues tested (*2*). Homologs of BH which also have peptidase activities have been identified in yeast (*4*, *5*) and bacteria (*6*). The yeast BH has 35 percent amino acid identity with the bacterial forms (PepC) and 43 percent identity with the available partial cDNA sequence of the mammalian BH (276 of ~450 amino acids), implying an evolutionarily conserved role from bacteria to mammals for this peptidase activity. As in mammalian cancer cells, over-expression of the yeast BH in yeast confers increased resistance to bleomycin (*4*, *5*).

The yeast form of BH was unexpectedly purified as a DNA-binding protein that binds to upstream activating sequences (UAS_G) of the GAL system (*4*). The 454-residue protein preferentially binds single-stranded DNA (K_d~10 nM) over double-stranded (K_d~1 μM). Further, the amounts of BH protein in yeast BH are regulated by the Gal4 regulatory protein, prompting the designation of the gene encoding yeast BH as *GAL6* (*4*). Gal4 is a positive regulatory protein that has a central role in the control of gene expression in the galactose metabolism system of yeast. Gal4 and the *GAL* genes it controls serve as a model system for studying eukaryotic gene regulation (*7*). Gal4 regulates *GAL6* expression by binding a site in the promoter of *GAL6*. Gal6 itself apparently negatively regulates *GAL* gene expression and when *GAL6* is deleted, the levels of the *GAL* gene RNA become three to five times higher (*8*). Thus, Gal6 appears to be part of a negative feedback regulatory system in yeast, adding another dimension to the cellular roles of BH.

The BHs apparently have cellular functions that have been conserved from bacteria to humans. Presumably these functions involve both proteolysis and DNA binding. We now describe the three-dimensional structure of Gal6. Unlike many bifunctional proteins, the DNA-binding and protease activities of Gal6 are intimately intertwined at both the tertiary and quaternary structural levels with an organization strikingly analogous to that of the 20S proteasome (*9*). This feature may be key to understanding the conserved cellular functions of this

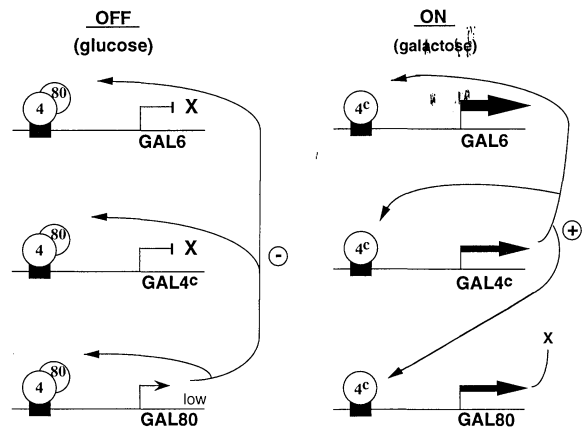

Fig. 1. A general system for the overproduction of proteins in yeast as applied to Gal6. The target gene (*GAL6*) is under control of a Gal4 responsive promoter (*GAL1*) and is on a multicopy plasmid. Gal4 is a positive regulatory protein that is repressed by Gal80 protein, which is also under Gal4 transcriptional control. A mutant form of Gal4, $Gal4^c$, is also under Gal4 regulation. In the absence of the inducer, galactose, there is no expression of the target gene or of the $GAL4^c$ gene. On induction, the *GAL6* gene is expressed. Its expression is maximized by overexpression of the $Gal4^c$ protein, which is not subject to repression by Gal80 protein and saturates the Gal6 promoter sites. In this system, a modification of earlier ones (*39*, *40*), the target protein is produced in a eukaryotic host; expression of the target protein is completely repressed until induction, allowing production of toxic proteins; the negative feedback regulation of the Gal80 protein (which is required to keep the system off until induction) is bypassed after induction by overproduction of the mutant $Gal4^c$ protein. When applied to Gal6, protein production saturates 4 to 6 hours after induction, with Gal6 comprising 5 to 10 percent of the total cellular protein (the most abundant protein band in total cell extracts). The yeast strain stops growing, presumably because of overproduction of the protein. Gal6 protein was purified after induction by conventional chromatography (*4*) to more than 98 percent purity.